

Supplementary Material

1 SUPPLEMENTARY FIGURES

1.1 Figures

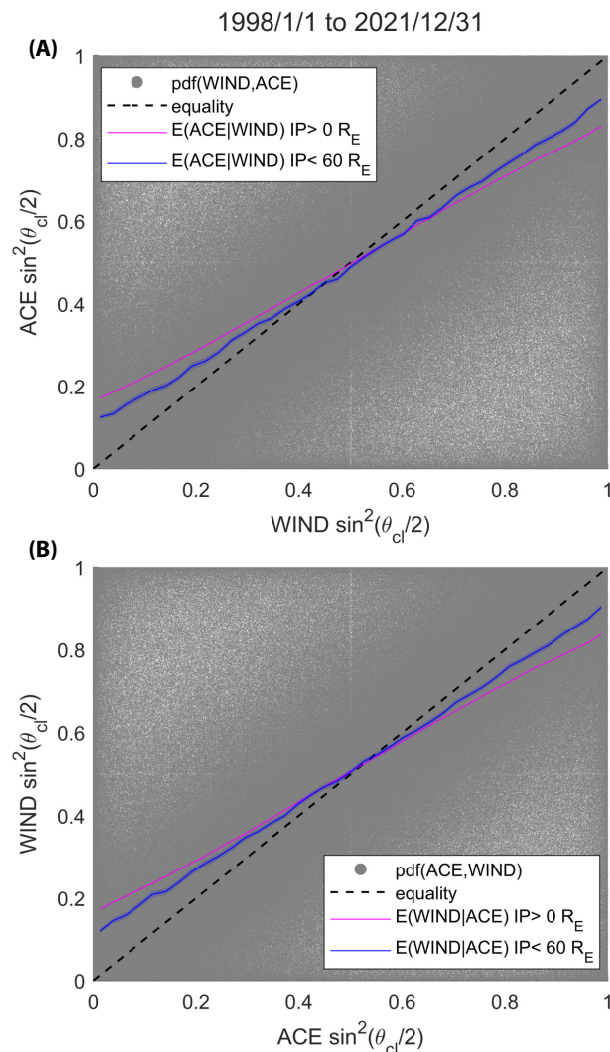


Figure S1. Regression bias in a function of Solar Wind IMF Clock Angle: $\sin^2(\theta_{cl}/2)$. **(A)** Regression function $E(\sin^2(\theta_{cl}^{ACE}/2) | \sin^2(\theta_{cl}^{WIND}/2))$ is shown with the magenta line. Blue line plots the same with only measurements where ACE and WIND have an impact parameter less than $60R_E$. **(B)** Shows the regression function $E(\sin^2(\theta_{cl}^{WIND}/2) | \sin^2(\theta_{cl}^{ACE}/2))$ using the magenta line. Blue line plots the same regression function for measurements with an IP less than $60R_E$. The regression functions are biased with a lower slope, however when both spacecraft measure similar solar wind the bias is not as high.

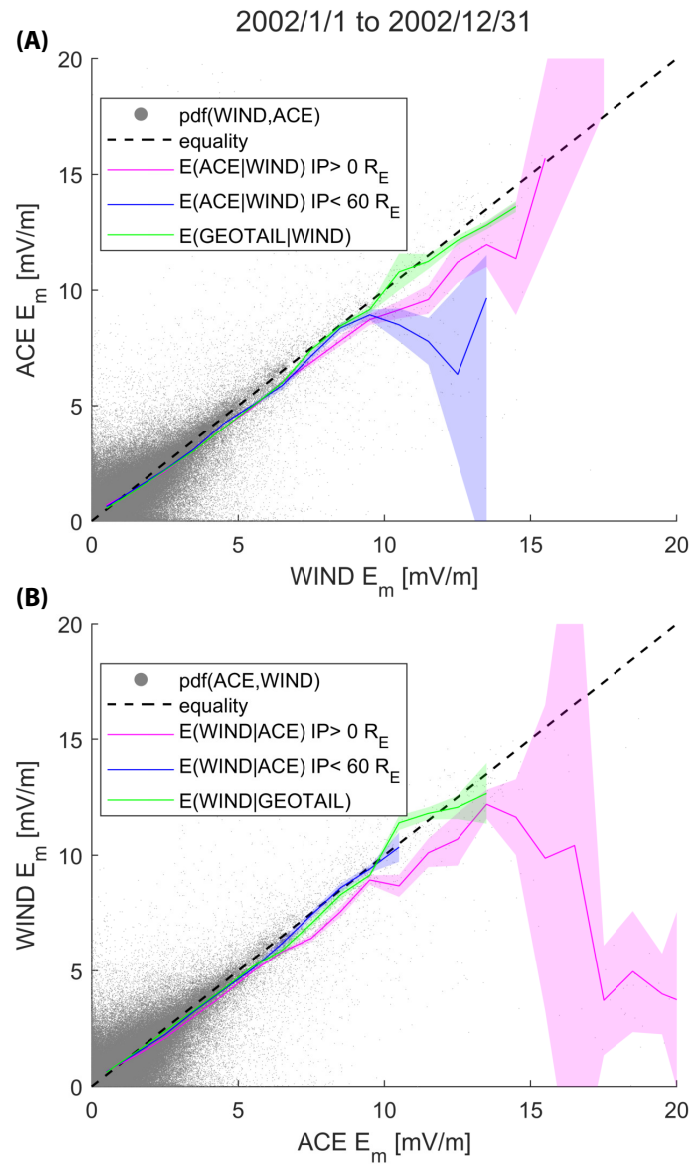


Figure S2. Regression bias in the merging electric field $E_m = V_{sw} B_T \sin^2(\theta_{cl}/2)$. **(A)** The magenta line plots the regression function $E(E_m^{ACE} | E_m^{WIND})$ using measurements in 2002. The blue line is the same but limited to measurements where the IP < 60 R_E between ACE and WIND. **(B)** Plots the reverse regression function $E(E_m^{WIND} | E_m^{ACE})$ in magenta, and the same curve with IP < 60 R_E between the spacecrafts. Note that the regression bias at extreme values here is a result of the fact that the IP between WIND and ACE were as large $\sim 265 R_E$.